2014

Robust and Dynamically Consistent Model Order Reduction for Nonlinear Dynamic Systems

David B. Segala

David Chelidze
University of Rhode Island, chelidze@uri.edu

Citation/Publisher Attribution
Segala, D. B., & Cheldize, D. (2014). Robust and dynamically consistent model order reduction for nonlinear dynamic systems. *Journal of Dynamic Systems, Measurement, and Control, 137*(2). 1-8. doi: 10.1115/1.4028470
Available at: http://dx.doi.org/10.1115/1.4028470

Robust and Dynamically Consistent Model Order Reduction for Nonlinear Dynamic Systems

David B. Segala[1]
Naval Undersea Warfare Center,
1176 Howell Street,
Newport, RI 02841
e-mail: david.segala@navy.mil

David Chelidze
Department of Mechanical Engineering,
University of Rhode Island,
Kingston, RI 02881
e-mail: chelidze@egr.uri.edu

There is a great importance for faithful reduced order models (ROMs) that are valid over a range of system parameters and initial conditions. In this paper, we demonstrate through two nonlinear dynamic models (pinned–pinned beam and thin plate) that are both randomly and periodically forced that smooth orthogonal decomposition (SOD)-based ROMs are valid over a wide operating range of system parameters and initial conditions when compared to proper orthogonal decomposition (POD)-based ROMs. Two new concepts of subspace robustness—the ROM is valid over a range of initial conditions, forcing functions, and system parameters—and dynamical consistency—the ROM embeds the nonlinear manifold—are used to show that SOD, as opposed to POD, can capture the low order dynamics of a particular system even if the system parameters or initial conditions are perturbed from the design case. [DOI: 10.1115/1.4028470]

1 Introduction

ROMs are having a greater impact with the increasing and advancing computing technologies. These advances in computing technologies that allow one to numerically interrogate larger scale, more complex dynamical systems (i.e., structural dynamics and acoustics, computational oceanographic/atmospheric dynamics, molecular dynamics, and rationale drug template design) for longer time periods and across multiple temporal and spatial scales.

A goal across the low order modeling community is to develop a ROM that is valid over an appropriate range of initial conditions, system parameters, and forcing functions. If the ROM is robust enough to yield faithful results over these ranges then the ROM has successfully captured or embedded the nonlinear manifold of the particular system of interest.

However, the following two questions still remain on the topic of ROMs: (1) "What is the lowest dimensional ROM?" and (2) "How well does the ROM capture the dynamics of the full scale system model or a perturbed version of that model?" Using the newly developed concepts of *subspace robustness* and *dynamical consistency*, the authors demonstrate through a periodically and randomly forced pinned–pinned beam and flat thin plate that SOD-based ROMs develop both dynamically consistent and robust ROMs as compared to POD-based ROMs.

2 Background

The approach for model reduction of linear and nonlinear systems is achieved in two different ways. For the sake of completeness, the methodology for linear systems will be briefly mentioned. Given a set of equations describing a linear dynamical system, one projects the equations onto a set of basis vectors obtained through some empirical methods. These methods can include linear normal modes (LNMs), Kyrlov subspaces, and POD [1–6] (also known as singular value decomposition [2], principal component analysis [2,7], and Karhunen–Loeve Decomposition [2,8]).

Model reduction for nonlinear systems is a much harder problem and currently the topic of many investigations. Some of these investigations have yielded techniques such as inertial manifold approximation, bilinearization about the equilibrium point, center manifold theory, nonlinear normal modes (NNMs), and POD. Thorough reviews can be found in Refs. [9–13].

Due to the scope of this paper, we will focus on the methodology which develops ROMs by taking the nonlinear system and projecting it onto a linear subspace spanned by a set of appropriate basis vectors. One such common set of basis vector is proper orthogonal mode (POM). In the formulation of POD, we seek to find a set of orthogonal subspaces that maximize the variance of its projections. These subspaces may miss the dominant mode if the system is randomly forced or there are perturbations to the system parameters which cause changes in energy levels. However, if the goal were to find a set of orthogonal subspaces that would maximize the overall smoothness of the projections, which would not rely on energy alone, the formulation would lead to SOD.

The multivariate multiscale data analysis method of SOD is proposed to find linear subspaces that fully embed the nonlinear manifold in an efficient low dimensional subspace. SOD can be thought of as an extension of POD [14–21]. In addition to considering spatial (i.e., statistical) characteristics of the data set as in POD, SOD considers temporal (i.e., dynamical) characteristics of the data set as well. In particular, SOD identifies coordinates (smooth orthogonal coordinates—SOCs) that have both minimal temporal roughness and maximal spatial variance. Therefore, SOD obtains the smoothest low dimensional approximation of a high dimensional system.

2.1 Proper and Smooth Orthogonal Decomposition.

Consider a dynamical system of which n state variables are measured. In addition, each n variable is sampled m times, which are arranged into a $m \times n$ ensemble matrix Y. If the n state variables are measurements at n spatial locations, then the Y_{ij} element represents the ith time instant value for the jth spatial location.

Next, an ensemble of time derivatives for each of the state variables is formed. These time derivatives can be available directly like in our case of model reduction, or given by $\dot{Y} \sim DY$ where D is some discrete differential operator (e.g., based on forward difference).

[1]Corresponding author.

Contributed by the Dynamic Systems Division of ASME for publication in the Journal of Dynamic Systems, Measurement, and Control. Manuscript received January 30, 2014; final manuscript received August 24, 2014; published online September 24, 2014. Assoc. Editor: Prashant Mehta.

Provided that Y and $\dot{Y}$ are zero mean, the autocovariance matrices can be formed by

$$\Sigma_{yy} = \frac{1}{m-1} Y^{\mathrm{T}} Y, \quad \Sigma_{\dot{y}\dot{y}} = \frac{1}{m-1} \dot{Y}^{\mathrm{T}} \dot{Y} \tag{1}$$

In the solution of POD, one tries to maximize the variance of the scalar field, Y. This is achieved by solving the eigenvalue problem of autocovariance matrix Σ_{yy} in Eq. (1)

$$\Sigma_{yy} \phi_k = \lambda_k \phi_k \tag{2}$$

where λ_k are proper orthogonal values (POVs), ϕ_k are POMs, and proper orthogonal coordinates (POCs) are $q = \Phi^{\mathrm{T}} Y$ where $\Phi = [\phi_1, \phi_2, \ldots, \phi_n] \in \mathbb{R}^n$. POVs are ordered such that $\lambda_1 \geq \lambda_2 \geq \ldots \lambda_n$. In practice, the solution for solving POD is achieved using singular value decomposition on the matrix Y.

Likewise, in the solution of SOD, one tries to not only maximize the variance of the scalar field, Y, but also minimize the local fluctuations of Y. Minimizing the local fluctuations is accomplished by minimizing the variance in the time derivative of the scalar field, $\dot{Y}$. This is achieved by solving the generalized eigenvalue problem of the matrix pair Σ_{yy} and $\Sigma_{\dot{y}\dot{y}}$ in Eq. (1)

$$\Sigma_{yy} \psi_k = \lambda_k \Sigma_{\dot{y}\dot{y}} \psi_k \tag{3}$$

where λ_k are now smooth orthogonal values (SOVs), $\psi_k \in \mathbb{R}^n$ are smooth projection modes (SPMs), smooth orthogonal modes (SOMs) are $\Phi = \Psi^{-\mathrm{T}}$, and SOCs are given by $q = \Psi Y$ where $\Psi = [\psi_1, \psi_2, \ldots, \psi_n] \in \mathbb{R}^n$. It should be noted that if we were to replace $\Sigma_{\dot{y}\dot{y}}$ with the identity matrix, then the formulation would yield the POD. In practice, especially if Y is ill-conditioned, the solution for solving SOD is achieved using generalized singular value decomposition on the matrix pair Y and DY.

3 Nonlinear Model Reduction

Consider the general class of nonlinear ordinary and differential equations described as

$$M\ddot{x} + C\dot{x} + Kx = F(\dot{x}, x, t) \tag{4}$$

where $x \in \mathbb{R}^n$ is a dynamic state variable, t is time, $M, C, K \in \mathbb{R}^{nxn}$ are the global mass, damping, and stiffness matrices, respectively, and $F \in \mathbb{R}^n$ describes any nonlinear forcing components. Using a coordinate transformation of $x = Pq$ where $q \in \mathbb{R}^k$ where $k \ll n$ is a reduced state variable and $P = [e_1, e_2, \ldots, e_n]$ is an appropriate set of basis vectors obtained through some empirical methods (e.g., POD or SOD), the corresponding ROM is

$$P^{\mathrm{T}} MP\ddot{q} + P^{\mathrm{T}} CP\dot{q} + P^{\mathrm{T}} KPq = P^{\mathrm{T}} F(P\dot{q}, Pq, t) \tag{5}$$

4 Model Reduction Subspace Selection

The purpose of this paper is to show that using SOD one can develop robust ROMs that embed the active nonlinear manifold as compared to POD. This is demonstrated using the newly developed concepts of *subspace robustness* and *dynamical consistency*. In Refs. [20,22], the authors describe two criteria in choosing an appropriate subspace for model order reduction, the selected subspace needs to: (1) embed or capture the active NNM manifold and (2) be insensitive to a varying set of initial conditions, system parameters, and forcing functions.

4.1 Subspace Robustness. The key idea behind subspace robustness is a quantitative metric that determines whether the subspace will be insensitive to perturbations of the system parameters and initial conditions. If a subspace is insensitive to these perturbations (e.g., off-design configurations), the subspace will still provide a faithful ROM of the system of interest.

Therefore, a subspace spanned by the basis vectors for model order reduction needs to be insensitive to variations in forcing functions, initial conditions, and system parameters. Conventional choices like POMs would be a good choice but they can vary with initial conditions, system parameters, and forcing functions [23]. Therefore, a decomposition identifies a *robust subspace* if all subspaces estimated from trajectories starting from different initial conditions and/or perturbed system parameters are mutually and nearly linearly dependent.

Given a matrix $S \in \mathbb{R}^{n \times ks}$ whose columns contain a set of basis vectors $\{P_i^k\}_{i=1}^s$ for each k-dimensional subspace, the corresponding *subspace robustness* γ_s^k is given by the following expression:

$$\gamma_s^k = \left| 1 - \frac{4}{\pi} \arctan \sqrt{\frac{\sum_{i=k+1}^{n} \sigma_i^2}{\sum_{i=1}^{k} \sigma_i^2}} \right| \tag{6}$$

From Eq. (6), if $\gamma_s^k = 0$ then the individual subspace realizations $P_i^k (i = 1, \ldots, s)$ are mutually linearly dependent. However, if $\gamma_s^k = 1$ then the individual subspace realizations are mutually linearly independent. Therefore, the subspace identified through some empirical procedure can only be used for model reduction if its subspace robustness γ_s^k is close to unity. Otherwise, that subspace may not capture all the needed system dynamics for particular sets of parameters.

4.2 Dynamical Consistency. The idea behind dynamical consistency stems from the idea of *false nearest neighbors* [24]—which determines how many dimensions are needed, in phase space, such that your trajectory does not intersect with itself. If there are no intersections (singularities), then two neighboring points on the trajectory are neighbors because of the dynamics and not due to projection. If a particular subspace creates a trajectory that contains zero false nearest neighbors, then that subspace fully captures the dynamics (i.e., embeds the nonlinear manifold). From a mathematical perspective, dynamical consistency is determined by estimating a ratio of the number of false nearest neighbors over the total number of nearest neighbor pairs in a particular k-dimensional subspace

$$\zeta^k = 1 - \frac{N_{fnm}^k}{N_{nm}} \tag{7}$$

where N_{fnm}^k is the estimated number of false nearest neighbors in a k-dimensional subspace and N_{nm} is the total number of nearest neighbor pairs used in the estimation. If ζ^k is close to unity, then that k-dimensional subspace is dynamically consistent.

N_{fnm}^k is estimated by comparing the distance between the temporally uncorrelated nearest neighbors in a k-dimensional space to the same distance in the $k+1$-dimensional space. If the change in the distances is one order of magnitude larger than the original k-dimensional distance, then these points are denoted as false nearest neighbors in k-dimensional space.

5 Nonlinear Dynamical Systems

5.1 Simply Supported Pinned–Pinned Beam. The eighteen degree-of-freedom (DOF) pinned–pinned beam is shown in Fig. 1. The length of the beam is 0.6 m, height 0.001 m, width 015 m, Young's modulus is 10e9 N/m, and density is 7850 kg/m^3. The beam is discretized into nine Euler Bernoulli beam elements with two DOF (displacement and rotation) per node. The first and last nodes experience pinned boundary conditions. The steady-state simulation trajectory consisted of 100,000 points with the time step of 0.007. The equations of motion describing the

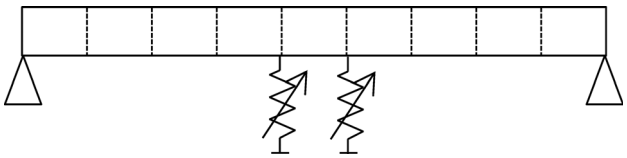

Fig. 1 A simply supported beam with two nonlinear springs positioned left and right of center

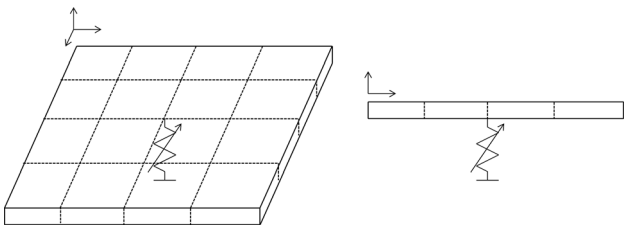

Fig. 2 A simply supported pate with a nonlinear spring positioned at the center node

dynamics of the beam are given by an 18-dimensional second-order equation which is described by Eq. (4), where $\mathbf{M} \in \mathbf{R}^{18\times18}$ is the global mass matrix, $\mathbf{K} \in \mathbf{R}^{18\times18}$ is the global stiffness matrix, $\mathbf{C} \in \mathbf{R}^{18\times18}$ is the global proportional damping matrix, and $F(x,\dot{x},t)$ can be decomposed into two terms: namely, $f_e(t)$ and $f_n(x)$. Two nonlinear springs whose nonlinear force $f_n(x)$ is described by Eq. (8) are positioned left and right of the center of the beam

$$f_n(x) = 3x - 8x^3 \tag{8}$$

For external forcing, a sine wave with frequency $\omega = 2\pi$ was chosen for the periodic forcing, $f_e(t) = f \sin \omega t$, and the random forcing was generated by interpolated random sequences. To generate the data for the subspace robustness, the model was simulated for four different forcing amplitudes, 0.1, 0.7, 1.3, and 2.0, where each was simulated using ten different initial conditions. This resulted in 40 different simulations.

5.2 Simply Supported Plate. The 78 DOF plate is shown in Fig. 2. The length of the plate is 10.0 m, thickens 0.1 m, width 10.0 m, Young's modulus is 30e6 N/m, shear correction factor is 5/6, Poisson's ratio is 0.3, and density is 7000 kg/m^3.

The plate is discretized into sixteen shear deformable plate elements with four nodes per element. Two-point integration is used for the bending term, while one-point integration is used for the shear. All the nodes on the perimeter of plate are simply supported. The steady-state simulation trajectory consisted of 100,000 points with the time step of 0.002. The equations of motion describing the dynamics of the plate are given by a 39-dimensional second-order equation described by Eq. (4). The matrices for the plate are $\mathbf{M} \in \mathbf{R}^{39\times39}$, $\mathbf{K} \in \mathbf{R}^{39\times39}$, $\mathbf{C} \in \mathbf{R}^{39\times39}$, and $F(x,\dot{x},t)$ can be decomposed into two terms: namely, $f_e(t)$ and $f_n(x)$. A nonlinear spring whose nonlinear force $f_n(x)$ is described by Eq. (9) is positioned at the center of the plate

$$f_n(x) = 4x - 8x^2 \tag{9}$$

For external forcing, a sine wave with frequency $\omega = 4\pi/5$ was chosen for the periodic forcing, $f_e(t) = f \sin \omega t$, and the random forcing was generated by interpolated random sequences. To generate the data for the subspace robustness, the model was simulated for four different forcing amplitudes, 50, 100, 150, and 200, where each was simulated using ten different initial conditions. This resulted in 40 different simulations.

6 Results

The subspace robustness for the beam is depicted in Fig. 3 (left) and for the plate in Fig. 4 (left). For the SOD-based ROM in both the periodically and randomly forced beam (◇ and ○, respectively), the similar trend can be observed. As the dimension is increased, the robustness increases monotonically until it reaches a value of unity at roughly a three-dimensional subspace. For both forcing cases in the plate model, there is a slight decrease in subspace robustness until a four-dimensional subspace is reached. Then, the trends increase monotonically until they reach a value of unity at roughly a ten-dimensional subspace. On the other hand, the robustness for the POD-based (▽ and □, respectively) subspaces do not exhibit a monotonically increasing trend. Actually, they seem to oscillate as the dimension is increased where they approach unity at some points but then rapidly decrease.

The dynamical consistency is depicted for the beam in Fig. 3 (right) and for the plate in Fig. 4 (right). For both forcing cases, the POD-based (▽ and □, respectively) and SOD-based (▽ and □, respectively) ROMs are similar in results. For the beam model, POD- and SOD-based ROMs are dynamically consistent in four dimensions or greater. In the plate model, they are consistent in three dimensions or greater. This suggests that both model order reduction techniques do provide subspaces which are dynamically consistent in equally low dimensional subspaces.

Figure 5 (left) shows the phase space trajectory for the eight DOF for the periodically forced beam with a forcing amplitude of $f = 1.0$ and frequency $\omega = 2\pi$. Figure 5 (right) depicts the

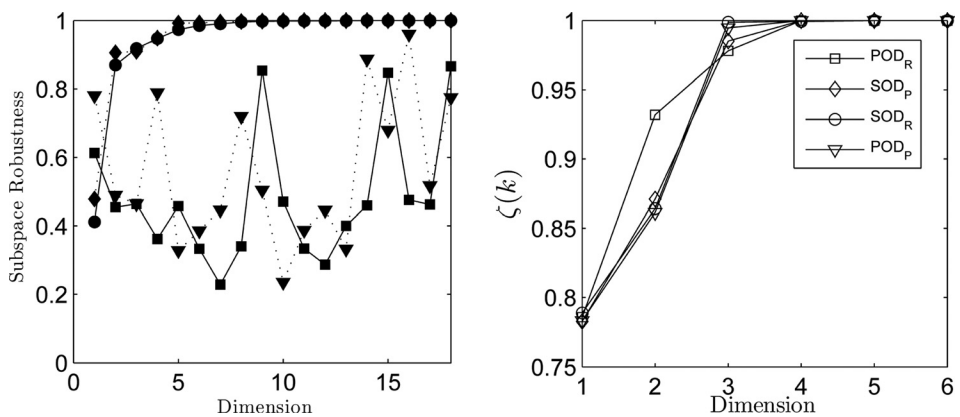

Fig. 3 (Left) Subspace robustness and (Right) dynamical consistency for both periodically and randomly forced POD-based (▽ and □, respectively) and SOD-based (◇ and ○, respectively) ROMs for the beam

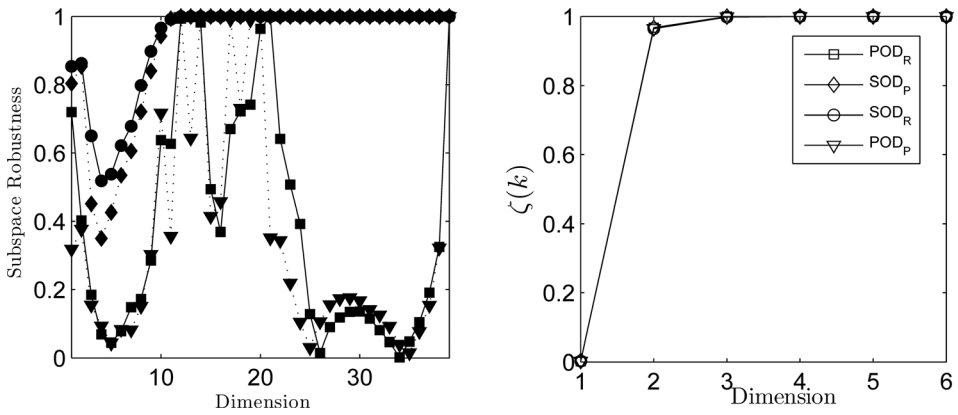

Fig. 4 (Left) Subspace robustness and (Right) dynamical consistency for both periodically and randomly forced POD-based (∇ and □, respectively) and SOD-based (◇ and ◯, respectively) ROMs for the plate

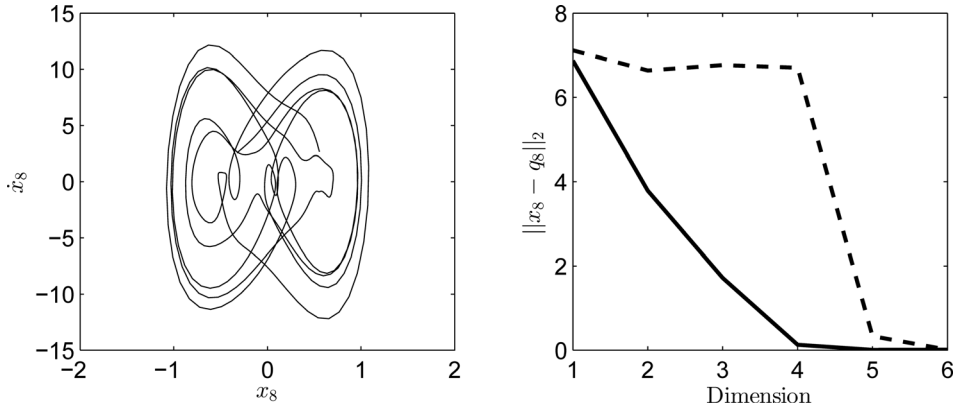

Fig. 5 (Left) Phase portrait for the eight DOF's full scale trajectory with periodic forcing with amplitude $f = 1.0$ for the beam that we wish to reconstruct. (Right) Corresponding L_2-norm between the full scale trajectory and the POD-based ROM (–) and the SOD-based ROM (- -) for the periodically forced beam.

corresponding L_2-norm between the full scale trajectory and the SOD (- -) and POD (–) based trajectory for increasing subspace dimension. POD-based ROM requires a four-dimensional subspace to reconstruct or track the phase space trajectories whereas SOD-based ROM requires six dimensions to completely reconstruct the same results.

Similar results can be drawn for the periodically forced plate as shown in Fig. 6. Here the plate is forced with an amplitude of $f = 100.0$ and frequency $\omega = 4\pi/5$. The plot on the left illustrates that phase portrait for the 21st DOF of the full scale system. Both two-dimensional POD- and SOD-based ROMs track the full scale dynamics quite well but a three-dimensional ROM fully captures the dynamics. If we consider a one-dimensional ROM, SOD captures the general structure whereas POD does not. This is reflected in the large difference in the first dimension for the corresponding L_2-norm.

The results for the randomly forced models are parallel to that of the periodically forced models. For the beam whose forcing amplitude is $f = 0.6$, a four-dimensional POD-based ROM captures the dynamics, whereas a five- or six-dimensional SOD-based ROM is needed, Fig. 7.

The results from the randomly forced plate with forcing amplitude $f = 100.0$ are shown in Fig. 8 where POD outperforms SOD-based ROMs. POD can capture the full scale dynamics better in all dimensions as compared to SOD until six dimensions where they both capture the dynamics.

Now, we can investigate how well the subspace extracted for model reduction from one set of system parameters and initial conditions approximates the full scale dynamics for a perturbed set of system parameters and initial conditions. For the periodically forced beam, the SOD- and POD-based subspaces were developed from the full scale dynamical system, which are excited with a forcing amplitude of $f = 2.0$ and a random initial condition. These extracted subspaces are now used to approximate the full scale dynamic model with forcing amplitude $f = 1.3$ and zeroes as the initial condition. The results are depicted in Fig. 9 where the full scale trajectory is shown for the off-design configuration that we wish to reconstruct. Using a one-dimensional subspace, POD outperforms SOD. However, in POD there are some added dynamics in the left lobe, which are not present in the full scale trajectory. In going to a two-dimensional subspace, SOD surpasses POD in almost fully capturing the dynamics. POD needs three dimensions to capture the same information.

The periodically forced plate is shown in Fig. 10 whose full scale dynamics are forced at a frequency of $\omega = 4\pi/5$ with a random initial condition. The ROM is developed for the model with frequency of $\omega = 3\pi/5$ and zeroes as the initial condition. SOD is able to fully capture the dynamics in six dimensions where the ROM is continually improved as dimensions are increased. Furthermore, SOD outperforms POD in each dimension. It is interesting to note that after a two-dimensional subspace, POD does not get any better with increasing dimension.

The randomly forced beam Fig. 11 is excited with a forcing amplitude of $f = 2.0$ and zeroes as the initial condition for both the full scale model and the ROM is used. However, the coefficient in front of the nonlinear spring term is changed from $\beta = 10$ to

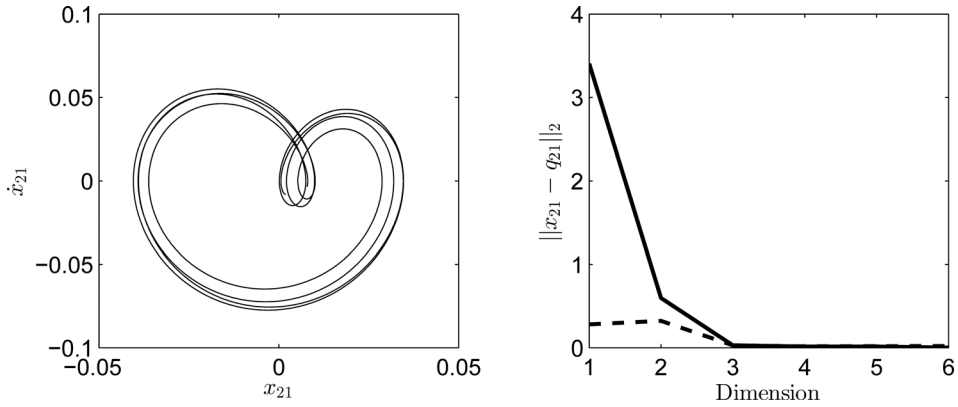

Fig. 6 (Left) Phase portrait for the 21st DOF's full scale trajectory with periodic forcing with amplitude $f = 100.0$ for the plate that we wish to reconstruct. (Right) Corresponding L_2-norm between the full scale trajectory and the POD-based ROM (–) and the SOD-based ROM (- -) for the periodically forced plate.

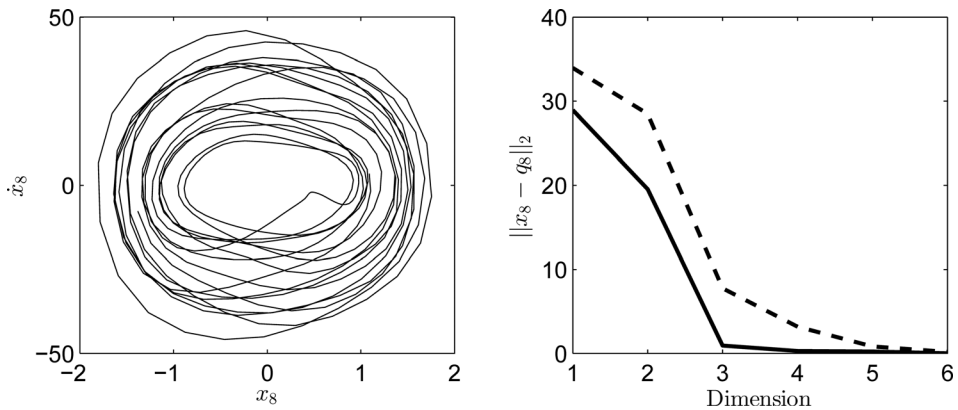

Fig. 7 (Left) Phase portrait for the eight DOF's full scale trajectory with random forcing with amplitude $f = 0.6$ for the beam that we wish to reconstruct. (Right) Corresponding L_2-norm between the full scale trajectory and the POD-based ROM (–) and the SOD-based ROM (- -) for the randomly forced beam.

$\beta = 5$. SOD is able to track the dynamics in a four-dimensional space which agrees with POD as well. However, the L_2-norm increases from a one- to a two-dimensional POD-based ROM. This further supports the subspace robustness which showed this exact result. In SOD, continual improvement is demonstrated with increasing dimension.

Finally, for the plate which is shown in Fig. 12, the full scale dynamical system which is excited with a random initial condition and a nonlinear spring coefficient $\beta = 16$. The extracted subspaces are now used to approximate the full scale dynamic model with zeroes as the initial condition and nonlinear spring coefficient $\beta = 8$. Both POD and SOD perform equally well in this case. In

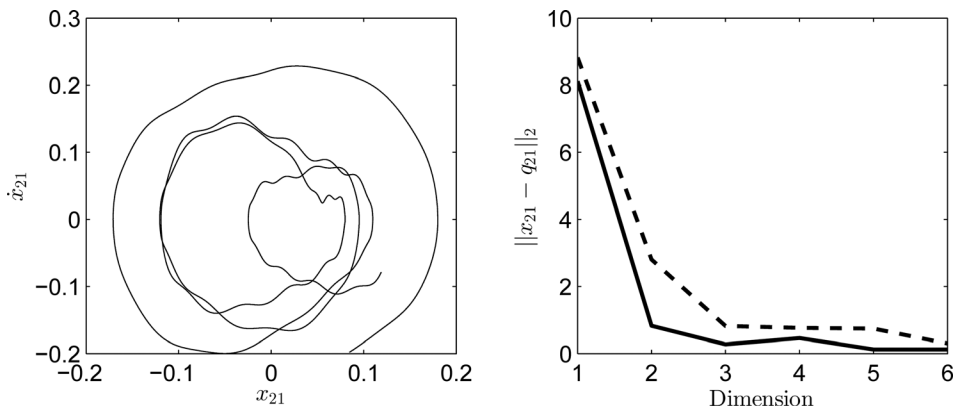

Fig. 8 (Left) Phase portrait for the 21st DOF's full scale trajectory with random forcing with amplitude $f = 100.0$ for the plate that we wish to reconstruct. (Right) Corresponding L_2-norm between the full scale trajectory and the POD-based ROM (–) and the SOD-based ROM (- -) for the randomly forced plate.

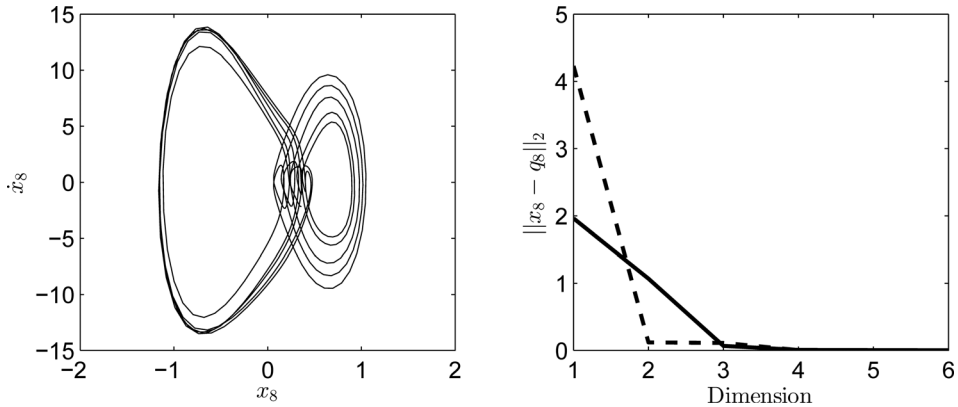

Fig. 9 (Left) Phase portrait for the eight DOF's full scale trajectory with periodic forcing with amplitude $f = 2.0$ and random initial condition for the beam that we wish to reconstruct. Subspaces were constructed with system parameters $f = 1.3$ and zeroes as the initial condition. (Right) Corresponding L_2-norm between the full scale trajectory and the POD-based ROM (–) and the SOD-based ROM (- -) for the periodically forced beam off-design configuration.

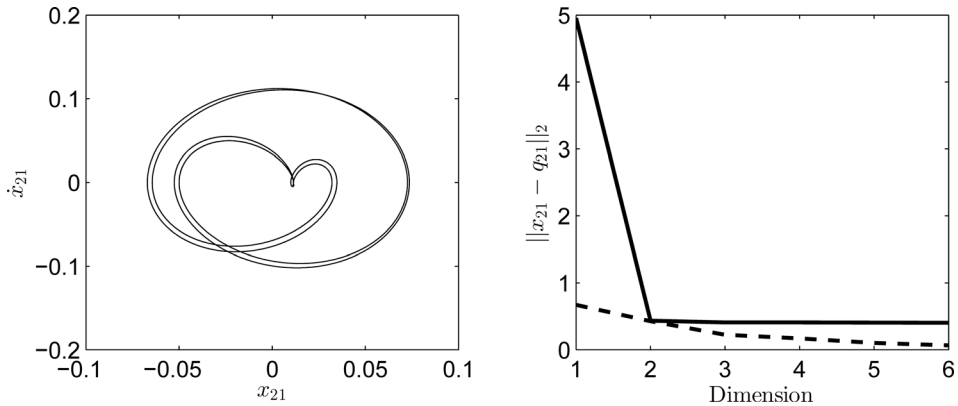

Fig. 10 (Left) Phase portrait for the 21st DOF's full scale trajectory with periodic forcing frequency of $\omega = 4\pi/5$ and a random initial condition for the plate that we wish to reconstruct. Subspaces were constructed with system parameters $\omega = 3\pi/5$ and zeroes as the initial condition. (Right) Corresponding L_2-norm between the full scale trajectory and the POD-based ROM (–) and the SOD-based ROM (- -) for the periodically forced plate.

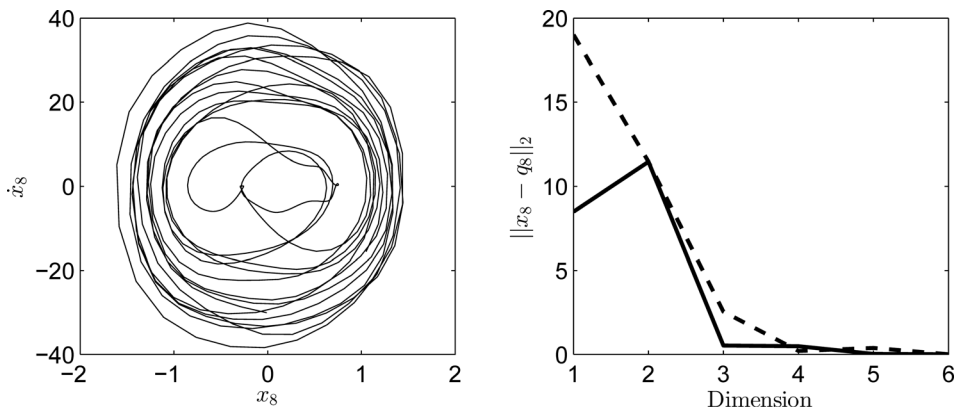

Fig. 11 (Left) Phase portrait for the eight DOF's full scale trajectory with zeroes as the initial condition and nonlinear spring coefficient $\beta = 10$ for the beam that we wish to reconstruct. Subspaces were constructed with system parameters zeroes as the initial condition and nonlinear spring coefficient $\beta = 5$. (Right) Corresponding L_2-norm between the full scale trajectory and the POD-based ROM (–) and the SOD-based ROM (- -) for the randomly forced beam off-design configuration.

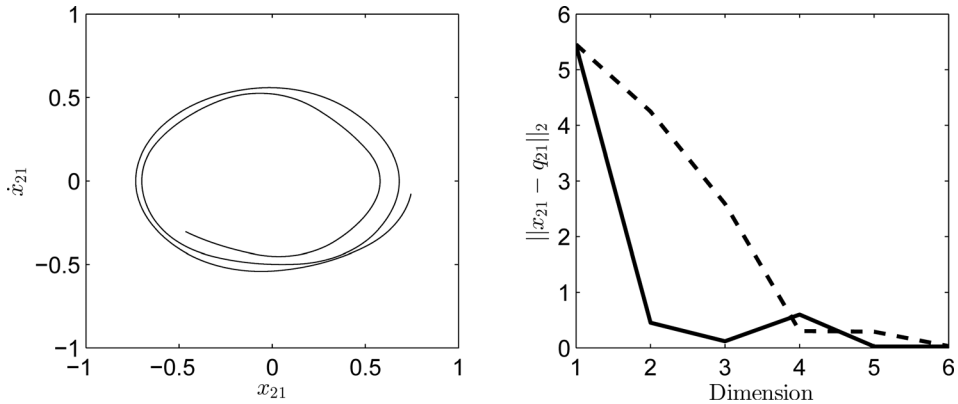

Fig. 12 (Left) Phase portrait for the 21st DOF's full scale trajectory with random initial condition and nonlinear spring coefficient $\beta = 16$ for the plate that we wish to reconstruct. Subspaces were constructed with system parameters zeroes as the initial condition and nonlinear spring coefficient $\beta = 8$. (Right) Corresponding L_2-norm between the full scale trajectory and the POD-based ROM (–) and the SOD-based ROM (- -) for the randomly forced plate.

fact, they both show continual improvement with increasing dimension and reconstruct the dynamics with a six-dimensional subspace.

7 Discussion

The purpose of this work was to show, using two new concepts of subspace robustness and dynamical consistency, that SOD-based ROMs are not only robust to perturbations of the system parameters but also embed the nonlinear manifold of a nonlinear dynamical system. This is demonstrated using an 18 DOF pinned–pinned beam supported by two nonlinear springs left and right of center and a 78 DOF plate with a nonlinear spring in the center.

For both the periodically and randomly forced beam and plate models, when the ROMs are created and compared against the same full scale dynamic models POD always outperforms SOD. By definition, POD tries to minimize the error in the projections in the least squares sense. Therefore, the subspace that POD captures is going to be the lowest dimensional subspace needed to capture the nonlinear manifold. In some instances, for example, the periodically forced plate in Fig. 6, SOD's performance is comparable to POD.

However, one particular goal in low order modeling is to develop a ROM that is valid over a range of operating conditions. If the ROM is only valid for the set of parameters and initial conditions that were used to create the ROM, a new ROM will have to be created for each new set of parameters and initial conditions. This negates the reason for the ROM since the full scale model will have to be simulated for at least a brief amount of time to create the projection modes. The amount of time is dependent on the nonlinearity, time step needed to capture the fundamental mode, etc.

The subspace robustness for the beam and plate indicates that SOD-based ROMs are robust across a set of perturbed system parameters, or off-design configurations. This can be observed by noting that the robustness trend approaches unity and stays at unity. For POD-based ROMs, the subspace robustness never reaches a value of unity, although it does come very close. However, a value near unity does not guarantee that by increasing your dimension by one, that your new subspace will be robust.

POD- and SOD-based ROMs for the beam and plate are dynamically consistent at the same dimension. This metric suggests that both methods require the same dimensional linear subspace such that the projections of the dynamics on this subspace yield trajectories that are unique (i.e., completely unfolded in phase space).

In all the examples when the projection modes are generated from a full scale model with a set of parameters but is then compared against a full scale model that has different system parameter values, initial conditions, or forcing functions, SOD outperforms POD. This further supports the results from the subspace robustness. Furthermore, SOD adds continual improvement in its ROMs. This can be observed in Figs. 7, 11, and 12 that plot the L_2-norm between the full-scale and reduced trajectories. As the dimension is increased, SOD always stays constant or decreases toward zero. However, using POD, the value can increase which suggests that the subspace captures less dynamics then the dimension prior. This is exactly in line with the subspace robustness plots.

This is due to the definition of POD and SOD. Again, in POD, we are looking for an orthogonal subspace such that the projections maximize the variance. If the data that are trying to be reconstructed are random (i.e., generated from random forcing), the dominant direction in the phase space becomes distorted. However, the direction remains constant when the data are deterministic (i.e., periodic forcing). On the other hand, SOD seeks to find a set of orthonormal subspaces that try to maximize the smoothness of the projections. As a result, random forcing or perturbations to system parameters which cause changes in energy levels have a much less effect irrespective of the dimensionality of the subspace.

8 Conclusion

A simply supported pinned–pinned beam with two nonlinear springs left and right of center and a simply supported plate with a nonlinear spring at the center were used to demonstrate SODs ability over POD to develop robust, faithful ROMs. Using the two newly developed concepts of subspace robustness and dynamical consistency, it was shown that SOD-based ROMs are valid over a wide range of system parameters, forcing functions, and initial conditions as compared to POD-based ROMs. Therefore, SOD is able to embed the nonlinear manifold of the dynamical system in a lower dimensional space than POD. Furthermore, SOD offers continual improvement of its ROM as the number of dimensions is increased until the ROM fully tracks the full scale dynamical trajectories.

Acknowledgment

David Segala would like to thank the Naval Undersea Warfare Center Division Newport Internal Investments and David Chelidze would like to thank the National Science Foundation under Grant No. 1100031.

Nomenclature

LNM = linear normal mode
NNM = nonlinear normal mode
POC = proper orthogonal coordinate

POD = proper orthogonal decomposition
POM = proper orthogonal modes
POV = proper orthogonal values
ROMs = reduced order model
SOC = smooth orthogonal coordinate
SOD = smooth orthogonal decomposition
SOM = smooth orthogonal modes
SOV = smooth orthogonal values
SPM = smooth projection mode

References

[1] Chatterjee, A., 2000, "An Introduction to the Proper Orthogonal Decomposition," Curr. Sci., **78**(7), pp. 808–817.
[2] Liang, Y. C., Lee, H. P., Lim, S. P., Lin, W. Z., Lee, K. H., and Wu, C. G., 2002, "Proper Orthogonal Decomposition and Its Applications—Part I: Theory," J. Sound Vib., **252**(3), pp. 527–544.
[3] Feeny, B. F., and Kappagantu, R., 1998, "On the Physical Interpretation of Proper Orthogonal Modes in Vibrations," J. Sound Vib., **211**(4), pp. 607–616.
[4] Volkwein, S., 2008, "Model Reduction Using Proper Orthogonal Decomposition, Lecture Notes," *Institute of Mathematics and Scientific Computing*, University of Graz, Graz, Austria.
[5] Kershen, G., Poncelet, F., and Golinval, J., 2007, "Physical Interpretation of Independent Component Analysis in Structural Dynamics," Mech. Syst. Signal Process., **21**(4), pp. 1567–1575.
[6] Feeny, B., 2002, "On the Proper Orthogonal Modes and Normal Modes of a Continuous Vibration System," J. Sound Vib., **124**(1), pp. 157–160.
[7] Shlens, J., 2005, A Tutorial on Principal Component Analysis, Institute for Nonlinear Science, University of California, San Diego, La Jolla, CA.
[8] Berkooz, G., Holmes, P., and Lumley, J. L., 1993, "The Proper Orthogonal Decomposition in the Analysis of Turbulent Flows," Annuals Rev. Fluid Mech., **25**(1), pp. 539–575.
[9] Rega, G., and Troger, H., 2005, "Dimension Reduction of Dynamical Systems: Methods, Models, Applications," Nonlinear Dyn., **41**(1–3), pp. 1–15.
[10] Shaw, S., and Pierre, C., 1994, "Normal Modes of Vibration for Non-Linear Continuous Systems," J. Sound Vib., **169**(3), pp. 319–347.
[11] Shaw, S., and Pierre, C., 1991, "Non-Linear Normal Modes and Invariant Manifolds," J. Sound Vib., **150**(1), pp. 170–173.
[12] Shaw, S., and Pierre, C., 1993, "Normal Modes for Non-Linear Vibratory Systems," J. Sound Vib., **164**(1), pp. 85–124.
[13] Vakakis, A., 1997, "Non-Linear Normal Modes (NNMS) and Their Application in Vibration Theory: An Overview," Mech. Syst. Signal Process., **11**(1), pp. 3–22.
[14] Chelidze, D., and Liu, M., 2005, "Dynamical Systems Approach to Fatigue Damage Identification," J. Sound Vib., **281**(3–5), pp. 887–904.
[15] Chelidze, D., and Liu, M., 2008, "Reconstructing Slow-Time Dynamics From Fast-Time Measurements," Philos. Trans. R. Soc. A, **366**(1866), pp. 729–3087.
[16] Chelidze, D., and Cusumano, J. P., 2006, "Phase Space Warping: Nonlinear Time Series Analysis for Slowly Drifting Systems," Philos. Trans. R. Soc. A, **364**(1846), pp. 2495–2513.
[17] Chelidze, D., 2004, "Identifying Multidimensional Damage in a Hierarchical Dynamical System," Nonlinear Dyn., **310**(4), pp. 307–322.
[18] Chelidze, D., and Zhou, W., 2006, "Smooth Orthogonal Decomposition Based Modal Analysis," J. Sound Vib., **292**(3–5), pp. 461–473.
[19] Farooq, U., and Feeny, B., 2008, "Smooth Orthogonal Decomposition for Modal Analysis of Randomly Excited Systems," J. Sound Vib., **316**(1–5), pp. 137–146.
[20] Chelidze, D., 2013, "Smooth Robust Subspace Based Model Reduction," ASME Paper No. DETC2013-13333.
[21] Chelidze, D., 2009, "Nonlinear Normal Mode Embedding for Model Reduction," Euromech Colloquium 503: Nonlinear Normal Modes, Model Reduction and Localization, Frascati, Sept. 27–Oct. 2.
[22] Segala, D., and Chelidze, D., 2013, "Robust and Dynamically Consistent Reduced Order Models," ASME Paper No. IMECE2013-62522.
[23] Rathinam, M., and Petzold, L. R., 2003, "A New Look at Proper Orthogonal Decomposition," J. Numer. Anal., **41**(5), pp. 1893–1925.
[24] Kennel, M., Brown, R., and Abarbanel, H., 1992, "Determining Embedding Dimension for Phase-Space Reconstruction Using a Geometrical Construction," Phys. Rev. A, **45**(6), pp. 3403–3411.